

InN nanostructures
InN Nanocrystals, Nanowires, and Nanotubes

Kripasindhu Sardar, F. L. Deepak, A. Govindaraj,
 M. M. Seikh, and C. N. R. Rao*

Indium nitride has attracted increasing attention in the last few years because of its properties of potential value in optoelectronic devices and other technologies.^[1] There have been several efforts to prepare InN nanostructures, but the results reported are not altogether complete and satisfactory. Nanocrystals of InN have been produced by the reaction of InCl_3 and Li_3N at 250°C , but the material obtained was a mixture of the cubic and hexagonal phases.^[2] The reaction of In_2S_3 and NaNH_2 yielded hexagonal nanocrystals with diameters in the range of 10–30 nm, with an absorption band centered around 1.9 eV.^[3] Indium halide CVD on a Si(100) substrate in the presence of NH_3 has been used to produce flowerlike hexagonal crystals, but the size of the crystals is in the micrometer regime.^[4] In the decomposition of azido precursors, a solution–liquid–solid (SLS) process gave rise to ≈ 20 nm diameter InN fibers which are polycrystalline.^[5] Decomposition of another azido precursor yielded InN whiskers of 10–200 nm diameter by the vapor–liquid–solid (VLS) process, but the optical properties of the whiskers have not been reported.^[6] InN nanowires have been grown on a gold-coated silicon substrate by the thermal evaporation of pure In metal in the presence of NH_3 . The nanowires had a diameter in the 40–80 nm range, with a broad emission peak at 1.85 eV.^[7] By employing a VLS route, in which a mixture of In_2O_3 and In metal was reacted with NH_3 at $\approx 700^\circ\text{C}$, nanowires with diameters in the 10–100 nm range were obtained, but the optical spectra are not reported.^[8] CVD with a mixture of In_2O_3 and In along with NH_3 on a Si/SiO₂ substrate coated with Au (20 nm thick), gave nanowires of 15–30 nm diameter with an absorption band at ≈ 1.85 eV.^[9] We notice that some of the procedures used to produce the InN nanostructures employ relatively high temperatures, which can give rise to defects or cause decomposition. Where low-temperature reactions have been employed, the optical properties reported are not in tune with the present understanding of the material. While most of the papers on InN nanostructures report the 1.9 eV absorption band as being characteristic of the material, it is now believed that the band characteristic of InN is in the near-

IR region.^[10–12] Because of the importance of InN as an electronic material, we considered it important to carry out a systematic investigation of the nanostructures produced at relatively low temperatures, with specific interest in the optical properties. In this communication, we report a study of the nanocrystals, nanowires, and nanotubes of InN prepared by new chemical routes. We also demonstrate that a band around 0.7 eV in the near-infrared region is truly characteristic of InN.

A typical TEM image of the InN nanocrystals obtained by the solvothermal reaction of tris(*N*-nitroso-phenylhydroxylamino)indium, $[\text{In}(\text{C}_6\text{H}_5\text{N}_2\text{O}_2)_3]$, and 1,1,1,3,3,3-hexamethyldisilazane (HMDS) in toluene at 265°C is shown in Figure 1 a. The image reveals nanocrystals with an aver-

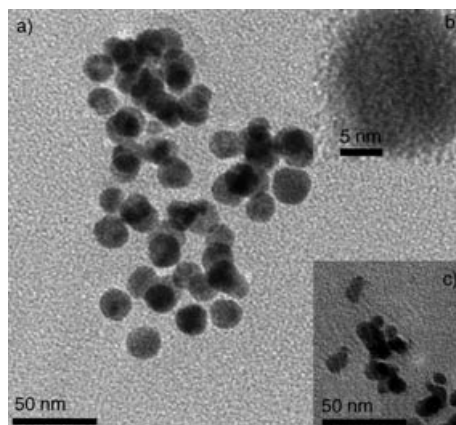


Figure 1. a) TEM image of InN nanocrystals prepared by the reaction of $[\text{In}(\text{C}_6\text{H}_5\text{N}_2\text{O}_2)_3]$ and HMDS; b) HREM image of one such nanocrystal; c) nanocrystals prepared by the reaction of InCl_3 and HMDS.

age diameter ≈ 15 nm. The nanocrystals are single-crystalline in nature, as evidenced from the high resolution electron microscope (HREM) image (Figure 1b). The lattice fringes correspond to the (101) plane of hexagonal InN with $d = 2.70$ Å. The reaction of InCl_3 with HMDS at 300°C also gave nanocrystals (diameter 10–15 nm; Figure 1c). The XRD pattern of the nanocrystals (Figure 2a) shows characteristic reflections of the wurtzite structure ($a = 3.56$ Å, $c = 5.70$ Å, JCPDS no.: 02-1450). The average particle size obtained from the Scherrer formula was ≈ 12 nm. The Raman spectra of the nanocrystals gave the characteristic bands due to the $A_1(\text{LO})$, E_2 , and $A_1(\text{TO})$ modes.^[3,13] In Figure 3a we show the optical absorption spectrum of the InN nanocrystals, which reveals a broad featureless absorption centered around 950 nm and a well-defined absorption band at ≈ 1575 nm (0.79 eV). The observation of the latter band in the near-infrared region is significant.

Reaction of indium acetate with HMDS in the absence of a solvent at 300°C yielded interesting nanostructures consisting of both nanowires and nanotubes with yields of 40 and 60%, respectively. The XRD pattern of these nanostructures was characteristic of wurtzite InN (Figure 2b). The SEM image in Figure 4a shows the presence of a large number of nanowires and nanotubes. The nanowires have diameters in the 50–100 nm range with lengths extending up to 1 μm , as seen in the low-resolution TEM images in Fig-

[*] K. Sardar, F. L. Deepak, Dr. A. Govindaraj, M. M. Seikh, Prof. Dr. C. N. R. Rao
 Chemistry and Physics of Materials Unit
 Jawaharlal Nehru Centre for Advanced Scientific Research
 Jakkur P.O., Bangalore 560064 (India)
 Fax: (+91) 80-2362-2760
 E-mail: cnrrao@jncasr.ac.in

K. Sardar, Dr. A. Govindaraj, M. M. Seikh, Prof. Dr. C. N. R. Rao
 Solid State and Structural Chemistry Unit
 Indian Institute of Science
 Bangalore 560012 (India)

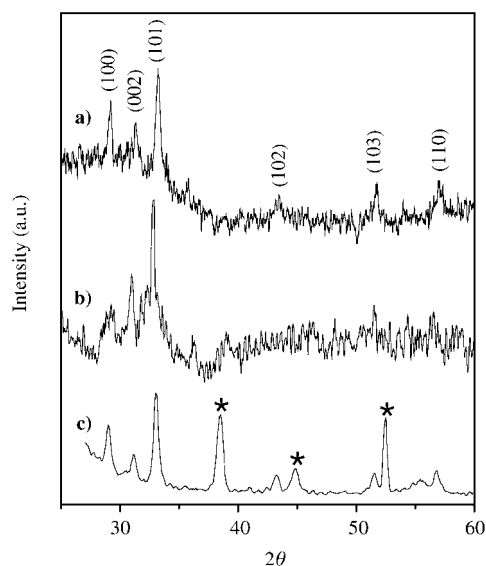


Figure 2. Powder XRD patterns: a) InN nanocrystals obtained from the reaction of $[\text{In}(\text{C}_6\text{H}_5\text{N}_2\text{O}_2)_3]$ and HMDS; b) a mixture of nanotubes and nanowires; c) InN nanowires obtained by NSP (grazing angle). Asterisks indicate peaks due to the Si(100) substrate.

ure 4b. We have also found the presence of a few Y-junction nanowires (Figure 4c). The nanowires are single-crystalline with Bragg spots corresponding to the (100), (101), and (002) planes in the selected-area electron diffraction (SAED) pattern (see inset of Figure 4c). HREM images of the nanowires gave interplanar spacings of $\approx 2.7 \text{ \AA}$, which corresponds to the (101) plane of the wurtzite structure, with the growth direction of the nanowires being parallel to the (101) plane. Figure 4d and e shows TEM images of the InN nanotubes. They show an interlayer spacing of 3.08 \AA corresponding to the (100) planes as shown in the HREM image in Figure 4f. This spacing is distinctly lower than the interlayer spacing of 3.4 \AA in carbon nanotubes. The inset in Figure 4f shows the SAED pattern of the InN nanotube

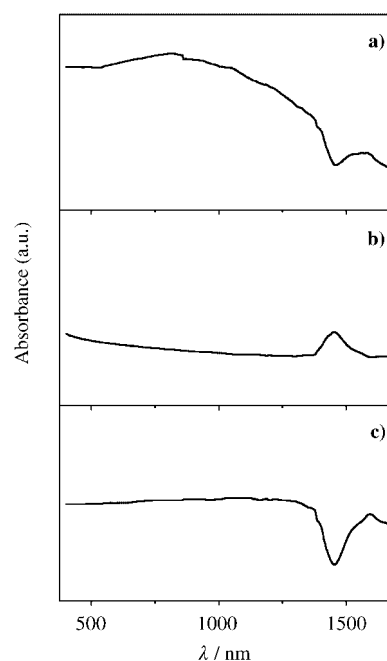


Figure 3. Electronic absorption spectra: a) InN nanocrystals; b) a mixture of InN nanowires and nanotubes (prepared by the reaction of indium acetate with HMDS); c) InN nanowires (prepared on a Si (100) substrate).



Editorial Advisory Board Member

C.N.R. Rao obtained his PhD from Purdue University and DSc from Mysore University. He is the Linus Pauling Research Professor and Honorary President of the J. Nehru Centre for Advanced Scientific Research and Honorary Professor at the Indian Institute of Science (both Bangalore). His research interests are mainly in solid-state and materials chemistry (e.g., transition-metal oxides, open-framework structures, and nanomaterials). He has authored nearly 1000 research papers and edited or written 30 books. A member of several academies including the Royal Society, US National Academy of Sciences, and the Pontifical Academy of Sciences, he is currently Distinguished Visiting Professor at the University of California, Santa Barbara. He recently received the Somya Award of the International Union of Materials Research Societies (IUMRS) and has also been awarded the Einstein Gold Medal of UNESCO and Hughes Medal of the Royal Society.

research papers and edited or written 30 books. A member of several academies including the Royal Society, US National Academy of Sciences, and the Pontifical Academy of Sciences, he is currently Distinguished Visiting Professor at the University of California, Santa Barbara. He recently received the Somya Award of the International Union of Materials Research Societies (IUMRS) and has also been awarded the Einstein Gold Medal of UNESCO and Hughes Medal of the Royal Society.

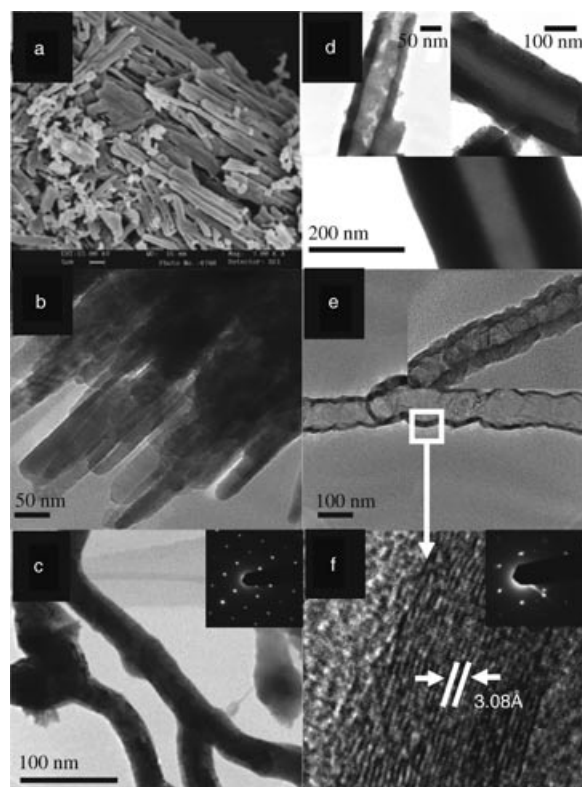


Figure 4. a) SEM image of a mixture of InN nanowires and nanotubes; b,c) TEM images of nanowires, d,e) TEM images of nanotubes; f) HREM image of a wall of the nanotube. The insets in (c) and (f) show the associated electron diffraction patterns.

with Bragg spots corresponding to the (100) planes. Optical absorption spectra of the nanowires and nanotubes gave a sharp band around 1475 nm (≈ 0.8 eV; Figure 3b). Interestingly, no distinct absorption features were found in the 600–1000 nm region.

We have also prepared single-crystalline InN nanowires by the reaction of indium acetylacetonate and NH_3 on Si(100) substrates covered with catalytic gold particles by employing the nebulized spray pyrolysis (NSP) technique.^[14] An SEM image (Figure 5a) reveals the high yield of nano-

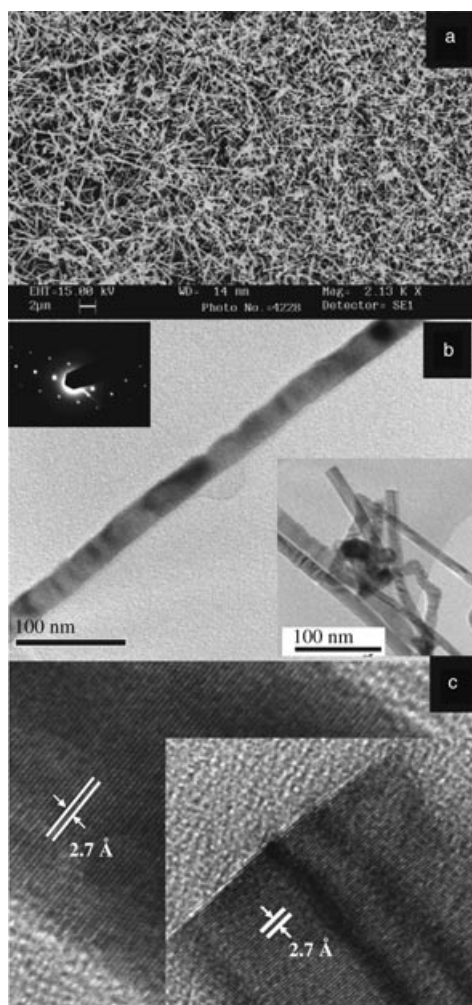


Figure 5. a) SEM image of the InN nanowires obtained by NSP; b,c) TEM and HREM images of the nanowires. The inset in (b) shows the SAED pattern and the inset in (c) shows the HREM image at the tip of the nanowire.

wires that are obtained. The grazing incidence XRD pattern of the nanowires (Figure 2c) is characteristic of the hexagonal structure, and the Raman spectrum is also characteristic of the wurtzite structure. TEM images (Figure 5b) show the nanowires to have diameters in the range of 10–40 nm, with lengths up to a few micrometers. The nanowires are single-crystalline, as proved by the SAED pattern (inset in Figure 5b), with spots corresponding to the (100), (002), and (101) planes. The HREM images in Figure 5c show lattice

fringes with a spacing of ≈ 2.70 Å corresponding to the (101) planes of the wurtzite structure. The growth of the nanowires is in the $\langle 101 \rangle$ direction. The HREM image of the tip of a nanowire shown as an inset in Figure 5c, does not contain any catalyst particle. The optical absorption spectrum of the InN nanowires (Figure 3c) shows a broad band in the ≈ 900 –1200 nm region, and a sharp feature around 1575 nm (0.79 eV).

The prepared InN nanocrystals, nanotubes, and nanowires all show a characteristic sharp band in the near-IR region (0.7–0.8 eV). This is significant since the nanocrystals and nanotubes were prepared at a low temperature (260–300°C), well below the decomposition temperature of InN (≈ 500 °C).^[15] The nanowires prepared at ≈ 585 °C also show the 0.8 eV band. We, therefore, propose that the 0.7 eV band is not due to an impurity, such as through the inclusion of metallic In.^[10] Wu et al.^[11a] have pointed out that the intrinsic bandgap in the 0.7–0.8 eV range is characteristic of InN rather than the commonly reported 1.9 eV. The variation of the bandgap between 0.7 and 1.7 eV is reported to arise as a result of the dependence on the electron concentration.^[11a–b] Theoretical calculations show that the intrinsic bandgap of InN is ≈ 0.65 eV.^[12] The 1.9 eV band has been considered to arise from oxygen incorporation.^[16] The absorption spectra reported in the present study clearly show that the band in the 0.7–0.8 eV region is exhibited by all the nanostructures of InN. Because of the absence of a clear band centered around 1.9 eV in the samples prepared by us at low temperatures, we have reason to believe that the 1.9 eV band may not be intrinsic, unlike the 0.7 eV band. Room-temperature PL emission spectra of all the InN nanostructures presented herein gave a band centered at around 675 nm (Figure 6), but we could not record the low-energy band in the near-infrared region. The 675 nm PL band arising from defects is known to be characteristic of InN.^[7,9] The infrared spectra of the nanostructures showed a band around 450 cm^{-1} due to In–N stretching mode.^[3]

In conclusion, InN nanocrystals, nanowires, and nanotubes have been successfully prepared by employing new

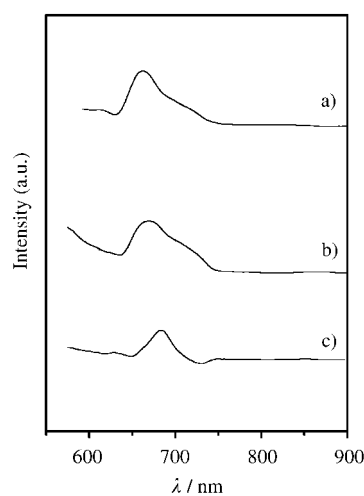


Figure 6. Photoluminescence spectra: a) InN nanocrystals; b) a mixture of InN nanowires and nanotubes; c) InN nanowires.

chemical routes. The nanostructures have been characterized by X-ray diffraction, electron microscopy, and various spectroscopic methods. It has been shown that the near-infrared band around 0.7 eV is characteristic of these materials.

Experimental Section

Indium cupferron ($[\text{In}(\text{C}_6\text{H}_5\text{N}_2\text{O}_2)_3]$) was prepared by the reaction of anhydrous InCl_3 (99.999%, Aldrich) and the ammonium salt of *N*-nitroso-*N*-phenylhydroxylamine ($\text{C}_6\text{H}_5\text{N}(\text{NO})\text{ONH}_4$, 97%, Aldrich) in a 1:3 molar ratio in deionized water at 0 °C. An instant precipitation was observed. The white precipitate was washed thoroughly with cold deionized water and then dried at room temperature. The white powder obtained was recrystallized from methanol and characterized by thermogravimetric analysis and infrared spectroscopy. $[\text{In}(\text{C}_6\text{H}_5\text{N}_2\text{O}_2)_3]$ (0.2 mmol) was dissolved in anhydrous toluene (10 mL). To the solution, 1,1,1,3,3,3-hexamethyldisilazane (HMDS; 5 mL, 99.9%, Aldrich) and *N*-cetyl-*N,N,N*-trimethylammonium bromide (CTAB; 0.3 mmol) was added. The mixture was stirred for 30 min and transferred to a stainless steel autoclave (25 mL capacity). The autoclave was kept inside an oven maintained at 265 °C. The reaction was carried out for 2–4 days to enhance the crystallinity of the material, although InN formation was complete within 6–12 h. The black-colored suspension obtained was centrifuged and the precipitate cleaned with absolute ethanol, and dispersed in toluene for further characterization.

To prepare InN nanocrystals starting from InCl_3 , anhydrous InCl_3 (0.23 mmole, 99.999%, Aldrich) was placed in the stainless steel autoclave (25 mL capacity) containing toluene (10 mL) and CTAB (0.15 mmole). To this solution, HMDS (5 mL) was added drop by drop and the mixture sonicated for 15 min. The autoclave was placed inside an oven maintained at 300 °C, and the reaction was carried out for between 6–96 h. InCl_3 forms a well-defined complex with HMDS at room temperature,^[17] which decomposes under solvothermal conditions to give the InN nanocrystals.

One-dimensional nanostructures of InN were obtained by the reaction of $\text{In}(\text{OAc})_3$ (0.5 mmole, 99.99%, Aldrich) and HMDS (5 mL) in a 25 mL stainless steel autoclave maintained in a furnace at a temperature of 300 °C for 48 h. No external solvent or surfactant was added and HMDS itself acted as the solvent. After the reaction was complete, the contents were cooled slowly to room temperature. The product was removed by filtration, washed with absolute ethanol and dried. The aspect ratio of these 1D nanostructures could be controlled by varying the relative reactant concentrations and temperature.

Nebulized spray pyrolysis (NSP) was employed to grow InN nanowires by the following procedure: A dilute solution (≈ 1 mM) containing indium acetylacetonate in methanol was atomized using a PZT transducer. The atomized vapor was passed over the Au-coated (≈ 50 Å) *n*-type Si(100) substrate maintained at 585 °C inside a quartz tube furnace in flowing NH_3 .

The nanostructures were characterized by powder X-ray diffraction (XRD) using $\text{Cu}_{\text{K}\alpha}$ radiation with a Rich-Seifert 3000-TT diffractometer. Scanning Electron Microscope (SEM) images were obtained with a LEICA S440i microscope. Transmission Electron

Microscopy (TEM) images were recorded with a JEOL JEM 3010 microscope operating at an accelerating voltage of 300 kV. Optical spectra were recorded at room temperature. Electronic absorption spectra were recorded using a Perkin-Elmer Lambda 900 UV/VIS/NIR spectrophotometer. The samples were dispersed in absolute ethanol or toluene and recorded in the 2000–200 nm range. Photoluminescence (PL) measurements were carried out with a Perkin-Elmer LS 50B luminescence spectrophotometer with an excitation wavelength of 520 nm. Infrared spectra were recorded with a Bruker FT-IR spectrometer. The Raman measurements were performed in a 90° geometry using a Jobin Yvon TRIAX 550 triple-grating spectrometer equipped with a cryogenic charge-coupled device camera, using a diode-pumped frequency-doubled solid-state Nd:YAG laser of 532 nm (Model DPSS 532-400, Coherent Inc. USA).

Keywords:

indium · nanocrystals · nanotubes · nanowires · nitrides

- [1] F. A. Ponce, D. P. Bour, *Nature* **1997**, *386*, 351–359.
- [2] Y.-J. Bai, Z.-G. Liu, X.-G. Xu, D.-L. Cui, X.-P. Hao, X. Feng, Q.-L. Wang, *J. Cryst. Growth* **2002**, *241*, 189–192.
- [3] J. Xiao, Y. Xie, R. Tang, W. Luo, *Inorg. Chem.* **2003**, *42*, 107–111.
- [4] N. Takahashi, A. Niwa, H. Sugiura, T. Nakamura, *Chem. Commun.* **2003**, 318–319.
- [5] S. D. Dingman, N. P. Rath, P. D. Markowitz, P. C. Gibbons, W. E. Buhro, *Angew. Chem.* **2000**, *112*, 1530–1532; *Angew. Chem. Int. Ed.* **2000**, *39*, 1470–1472.
- [6] H. Parala, A. Devi, F. Hipler, E. Maile, A. Birkner, H. W. Becker, R. A. Fischer, *J. Cryst. Growth* **2001**, *231*, 68–74.
- [7] C. H. Liang, L. C. Chen, J. S. Hwang, K. H. Chen, Y. T. Hung, Y. F. Chen, *Appl. Phys. Lett.* **2002**, *81*, 22–24.
- [8] J. Zhang, L. Zhang, X. Peng, X. Wang, *J. Mater. Chem.* **2002**, *12*, 802–804.
- [9] T. Tang, S. Han, W. Jin, X. Liu, C. Li, D. Zhang, C. Zhou, B. Chen, J. Han, M. Meyyappan, *J. Mater. Res.* **2004**, *19*, 423–426.
- [10] T. V. Shubina, S. V. Ivanov, V. N. Jmerik, D. D. Solnyshkov, V. A. Vekshin, P. S. Kopev, A. Vasson, J. Leymarie, A. Kavokin, H. Amano, K. Shimono, A. Kasic, B. Monemar, *Phys. Rev. Lett.* **2004**, *92*, 1174071–1174074.
- [11] a) J. Wu, W. Walukiewicz, K. M. Yu, J. W. Ager III, E. E. Haller, H. Lu, W. J. Schaff, Y. Saito, Y. Nanishi, *Appl. Phys. Lett.* **2002**, *80*, 3967–3969; b) J. Wu, W. Walukiewicz, S. X. Li, R. Armitage, J. C. Ho, E. R. Weber, E. E. Haller, H. Lu, W. J. Schaff, A. Barcz, R. Jakiela, *Appl. Phys. Lett.* **2004**, *84*, 2805–2807.
- [12] F. Bechstedt, J. Furthmüller, *J. Cryst. Growth* **2002**, *246*, 315–319.
- [13] G. Kaczmarczyk, A. Kaschner, S. Reich, A. Hoffmann, C. Thomssen, D. J. As, A. P. Lima, D. Schikora, K. Lischka, R. Averbeck, H. Riechert, *Appl. Phys. Lett.* **2000**, *76*, 2122–2124.
- [14] A. R. Raju, H. N. Aiyer, C. N. R. Rao, *Chem. Mater.* **1995**, *7*, 225–231.
- [15] Q. Guo, O. Kato, A. Yoshida, *J. Appl. Phys.* **1993**, *73*, 7969–7971.
- [16] A. G. Bhuiyan, A. Hashimoto, A. Yamamoto, *J. Appl. Phys.* **2003**, *94*, 2779–2808.
- [17] S. T. Barry, D. S. Richeson, *Chem. Mater.* **1994**, *6*, 2220–2221.

Received: June 9, 2004

Published online on September 24, 2004